
Learning Deep Generative Models with Doubly Stochastic MCMC

Chao Du

Jun Zhu

Bo Zhang

Dept. of Comp. Sci. & Tech., State Key Lab of Intell. Tech. & Sys., TNList Lab,
Center for Bio-Inspired Computing Research, Tsinghua University, Beijing, 100084, China
du-c14@mails.tsinghua.edu.cn dcszj@mail.tsinghua.edu.cn dcszb@mail.tsinghua.edu.cn

Abstract

We present doubly stochastic gradient MCMC, a simple and generic method for (approximate) Bayesian inference of deep generative models in the collapsed continuous parameter space. At each MCMC sampling step, the algorithm randomly draws a mini-batch of data samples to estimate the gradient of log-posterior and further estimates the intractable expectation over latent variables via a Gibbs sampler or a neural adaptive importance sampler. We demonstrate the effectiveness on learning deep sigmoid belief networks (DSBNs). Compared to the state-of-the-art methods using Gibbs sampling with data augmentation, our algorithm is much more efficient and manages to learn DSBNs on large datasets.

1 Introduction

Learning deep models that consist of multi-layered representations has proven effective with state-of-the-art performance in many tasks [5, 13, 28]. To fit such deep models, a small dataset is often insufficient. Therefore, it is important to address the computational challenge of learning such deep models on large-scale datasets, which are often in high-dimensional spaces also. Deep generative models (DGMs) [13, 28] represent an important family of deep models that can answer a wide range of queries by performing probabilistic inference, such as inferring the missing values of input data, which is beyond the scope of recognition networks such as deep neural networks.

However, probabilistic inference with DGMs is challenging, especially when a Bayesian framework is employed, which is desirable as it can offer various possibilities, such as robustness to overfitting, sparse Bayesian inference [11] and nonparametric inference [1] to learn the graph structure. For Bayesian methods

in general, the posterior inference often involves intractable integrals because of several potential factors, such as that the space is extremely high-dimensional and that the Bayesian model is non-conjugate. To address the challenges, approximate methods have to be adopted, including variational [14, 30] and Markov chain Monte Carlo (MCMC) methods [27].

Although much progress has been made on stochastic variational methods for DGMs [16, 25], under some mean-field or parameterization assumptions, little work has been done on extending MCMC methods to learn DGMs in a Bayesian setting, which are often more accurate. A few exceptions exist. Gan et al. [11] present a Gibbs sampling for deep sigmoid belief networks with a sparsity-inducing prior via data augmentation, and Adams et al. [1] present a Metropolis-Hastings method for cascading Indian buffet process.

In this paper, we present a simple and generic method, named doubly stochastic gradient MCMC, to improve the efficiency of performing Bayesian inference on DGMs. By drawing samples in the collapsed parameter space, our method extends the recent work on stochastic gradient MCMC [32, 2, 24] to deal with the challenging task of posterior inference with DGMs. Besides the stochasticity of randomly drawing a mini-batch of samples in stochastic approximation, our algorithm introduces an extra dimension of stochasticity to estimate the intractable gradients by randomly drawing the latent variables in DGMs. The sampling can be done via a simple Gibbs sampler. We further develop a neural adaptive importance sampler, where the adaptive proposal is parameterized by a recognition network and the parameters are optimized by descending inclusive KL-divergence. By combining the two types of stochasticity, we construct an unbiased estimate of the gradient in the continuous parameter space. Then, a stochastic gradient MCMC method is applied with guarantee to (approximately) converge to the target posterior when the learning rates are set under some proper annealing scheme.

Our method can be widely applied to the DGMs with

either discrete or continuous latent variables. As an example, we demonstrate the efficacy on learning deep sigmoid belief networks on large-scale datasets, achieving significant speedup compared to the very recent Gibbs sampler with data augmentation [11].

Finally, note that independent from our work, Gan et al. [10] also adopted a Monte Carlo estimate via Gibbs sampling to the intractable gradients under a stochastic MCMC method particularly for topic models. Besides a general perspective which is applicable on various types of DGM models, we propose a neural adaptive importance sampler which is more efficient than Gibbs sampling and in most cases leads to better estimates.

2 Doubly Stochastic Gradient MCMC for Deep Generative Models

We now present the doubly stochastic gradient MCMC for deep generative models.

2.1 Variational MLE for DGMs

Let $\mathbf{X} = \{\mathbf{x}_n\}_{n=1}^N$ be a given dataset with N i.i.d. samples. A deep generative model (DGM) assumes that each $\mathbf{x}_n \in \mathbb{R}^J$ is generated from a vector of latent variables $\mathbf{z}_n \in \mathbb{R}^H$, which itself follows some distribution $p(\mathbf{z}|\boldsymbol{\alpha})$. Let $p(\mathbf{x}|\mathbf{z}, \boldsymbol{\beta})$ be the likelihood model. The joint probability of a DGM is as follows:

$$p(\mathbf{X}, \mathbf{Z}|\boldsymbol{\theta}) = \prod_{n=1}^N p(\mathbf{z}_n|\boldsymbol{\alpha})p(\mathbf{x}_n|\mathbf{z}_n, \boldsymbol{\beta}), \quad (1)$$

where $\boldsymbol{\theta} := (\boldsymbol{\alpha}, \boldsymbol{\beta})$. Depending on the structure of \mathbf{z} , e.g., directed or undirected graphs, various DGMs have been developed, such as deep belief networks [13], deep Boltzmann machines [28] and deep sigmoid belief networks [20], which are our focus in this paper.

Learning DGMs is often very challenging due to the intractability of posterior inference. The state-of-the-art methods resort to stochastic variational methods under the maximum likelihood estimation (MLE) framework, $\hat{\boldsymbol{\theta}} = \operatorname{argmax}_{\boldsymbol{\theta}} \log p(\mathbf{X}|\boldsymbol{\theta})$. Specifically, let $q_{\phi}(\mathbf{Z})$ be some variational distribution to approximate the true posterior $p(\mathbf{Z}|\mathbf{X}, \boldsymbol{\theta})$. A variational bound of the log-likelihood $\log p(\mathbf{X}|\boldsymbol{\theta})$ can be derived. Then, we optimize the variational bound with respect to the variational parameters. However, the variational bound is often intractable to compute analytically for DGMs. To address this challenge, one possible method is to bound the intractable parts with tractable ones by introducing extra variational parameters [30]; but these methods increase the gap between the bound being optimized and the log-likelihood, potentially leading to poorer estimates. Another way is to adopt the recent progress [16, 25, 20] on hybrid Monte Carlo and variational methods, which approximate the intractable

expectations and their gradients over the parameters $(\boldsymbol{\theta}, \phi)$ via some unbiased Monte Carlo estimates. Furthermore, to handle large-scale datasets, stochastic optimization [26, 7] of the variational objective can be used with a suitable learning rate annealing scheme. Note that variance reduction is a key part of these methods in order to have fast and stable convergence. The reweighted wake-sleep (RWS) [6] represents another type of methods that directly estimate the log-likelihood (as well as its gradient) via importance sampling, where the proposal distribution can be characterized by a recognition model (or inference network). We draw inspiration from these variational methods to build our MCMC samplers, as explained below.

2.2 Doubly Stochastic Gradient MCMC

We consider the Bayesian setting to infer the posterior distribution $p(\boldsymbol{\theta}, \mathbf{Z}|\mathbf{X}) \propto p_0(\boldsymbol{\theta})p(\mathbf{Z}|\boldsymbol{\theta})p(\mathbf{X}|\mathbf{Z}, \boldsymbol{\theta})$ or its marginal distribution $p(\boldsymbol{\theta}|\mathbf{X})$, by assuming some prior $p_0(\boldsymbol{\theta})$. Except a handful of special examples, the posterior distribution is intractable to infer. Though variational methods can be developed as in [16, 25, 20], under some mean-field or parameterization assumptions, they often require non-trivial model-specific deviations and may lead to inaccurate approximation when the assumptions are not properly made. Here, we consider MCMC methods, which are more generally applicable and can asymptotically approach the target posterior.

A straightforward application of MCMC methods can be Gibbs sampling or stochastic gradient MCMC [32, 2, 24]. However, a Gibbs sampler can suffer from the random-walk behavior in high-dimensional spaces. Furthermore, a Gibbs sampler would need to process all data at each iteration, which is prohibitive when dealing with large-scale datasets. The stochastic gradient MCMC methods can lead to significant speedup by exploring statistical redundancy in large datasets; but they require that the sample space is continuous, which is not true for many DGMs, such as deep sigmoid belief networks that have discrete latent variables. Below, we present a doubly stochastic gradient MCMC with general applicability.

We made the mildest assumption that the parameter space is continuous and the log joint distribution $\log p(\mathbf{x}, \mathbf{z}|\boldsymbol{\theta})$ is differentiable with respect to the model parameters $\boldsymbol{\theta}$ almost everywhere except a zero-mass set. Such an assumption is true for almost all existing DGMs. Then, our method draws samples in a collapsed space that involves the model parameters $\boldsymbol{\theta}$ only, by integrating out the latent variables \mathbf{z} :

$$p(\boldsymbol{\theta}|\mathbf{X}) = \frac{1}{p(\mathbf{X})} p_0(\boldsymbol{\theta}) \prod_{n=1}^N \int p(\mathbf{x}_n, \mathbf{z}_n|\boldsymbol{\theta}) d\mathbf{z}_n, \quad (2)$$

where for discrete variables the integral will be a summation. Then the gradient of the log-posterior is

$\nabla_{\boldsymbol{\theta}} \log p(\boldsymbol{\theta}|\mathbf{X}) = \nabla_{\boldsymbol{\theta}} \log p_0(\boldsymbol{\theta}) + \sum_{n=1}^N \nabla_{\boldsymbol{\theta}} \log p(\mathbf{x}_n|\boldsymbol{\theta})$, where the second term can be calculated as:

$$\begin{aligned} \nabla_{\boldsymbol{\theta}} \log p(\mathbf{x}|\boldsymbol{\theta}) &= \frac{1}{p(\mathbf{x}|\boldsymbol{\theta})} \frac{\partial}{\partial \boldsymbol{\theta}} \int p(\mathbf{x}, \mathbf{z}|\boldsymbol{\theta}) \, d\mathbf{z} \\ &= \int \frac{p(\mathbf{x}, \mathbf{z}|\boldsymbol{\theta})}{p(\mathbf{x}|\boldsymbol{\theta})} \frac{\partial}{\partial \boldsymbol{\theta}} \log p(\mathbf{x}, \mathbf{z}|\boldsymbol{\theta}) \, d\mathbf{z} \\ &= \mathbb{E}_{p(\mathbf{z}|\mathbf{x}, \boldsymbol{\theta})} \left[\frac{\partial}{\partial \boldsymbol{\theta}} \log p(\mathbf{x}, \mathbf{z}|\boldsymbol{\theta}) \right]. \end{aligned} \quad (3)$$

With the above gradient, we can adopt a stochastic gradient MCMC method to draw samples of $\boldsymbol{\theta}$. We consider the second-order stochastic gradient Hamiltonian Monte Carlo (SGHMC) [8]; but our method can be naturally extended to the first-order stochastic gradient Langevin dynamics [32] and stochastic gradient thermostats [9] algorithms. SGHMC defines a potential energy $U(\boldsymbol{\theta}) = -\log p(\boldsymbol{\theta})$ where $p(\boldsymbol{\theta})$ is the target distribution, and builds a Markov chain using the gradient of $U(\boldsymbol{\theta})$. In our case, the target distribution is $p(\boldsymbol{\theta}|\mathbf{X})$ and the gradient can be written as $\nabla_{\boldsymbol{\theta}} U(\boldsymbol{\theta}) = -\nabla_{\boldsymbol{\theta}} \log p_0(\boldsymbol{\theta}) - \sum_{n=1}^N \nabla_{\boldsymbol{\theta}} \log p(\mathbf{x}_n|\boldsymbol{\theta})$. Let B_t be a random mini-batch sampled from the training data \mathcal{D} . We get the SGHMC method:

$$\begin{aligned} \boldsymbol{\gamma}_{t,i} &= (1 - \xi)\boldsymbol{\gamma}_{t,i-1} + \lambda_t \left(\nabla \log p_0(\boldsymbol{\theta}_{t,i-1}) + \right. \\ &\quad \left. \frac{|D|}{|B_t|} \sum_{n \in B_t} \nabla \log p(\mathbf{x}_n|\boldsymbol{\theta}_{t,i-1}) \right) + \mathcal{N}(0, 2\xi\lambda_t) \\ \boldsymbol{\theta}_{t,i} &= \boldsymbol{\theta}_{t,i-1} + \boldsymbol{\gamma}_{t,i}, \end{aligned} \quad (4)$$

where $\boldsymbol{\gamma}_t$ are some augmented momentum variables, ξ is the momentum decay and the subscript i is the inner step of the discretization when simulating the Hamiltonian dynamic at iteration t . With a proper annealing scheme over the learning rate λ_t , the Hamiltonian dynamics will converge to the target posterior.

The remaining challenge is to compute the gradient as the expectation in Eq. (3) is often intractable for DGMs. Here, we construct an unbiased estimate of the gradient by a set of samples $\{\mathbf{z}^{(s)}\}_{s=1}^L$ from the posterior $p(\mathbf{z}|\mathbf{x}, \boldsymbol{\theta})$:

$$\nabla_{\boldsymbol{\theta}} \log p(\mathbf{x}|\boldsymbol{\theta}) \approx \frac{1}{L} \sum_{s=1}^L \left(\frac{\partial}{\partial \boldsymbol{\theta}} \log p(\mathbf{x}, \mathbf{z}^{(s)}|\boldsymbol{\theta}) \right). \quad (5)$$

To draw the samples $\mathbf{z}^{(s)}$, we consider two strategies. The first one is a Gibbs sampler, which alternately samples each dimension of \mathbf{z} given the others. A Gibbs sampler is simple and applicable to both discrete and continuous latent variables. The second strategy is neural adaptive importance sampling, which again applies to both discrete and continuous latent variables, as detailed below.

Let $q(\mathbf{z}|\mathbf{x}; \boldsymbol{\phi})$ be a proposal distribution which satisfies

$q(\mathbf{z}|\mathbf{x}; \boldsymbol{\phi}) > 0$ wherever $p(\mathbf{z}|\mathbf{x}, \boldsymbol{\theta}) > 0$, we then have

$$\nabla_{\boldsymbol{\theta}} \log p(\mathbf{x}|\boldsymbol{\theta}) = \mathbb{E}_{q(\mathbf{z}|\mathbf{x}; \boldsymbol{\phi})} \left[\frac{p(\mathbf{z}|\mathbf{x}, \boldsymbol{\theta})}{q(\mathbf{z}|\mathbf{x}; \boldsymbol{\phi})} \frac{\partial}{\partial \boldsymbol{\theta}} \log p(\mathbf{x}, \mathbf{z}|\boldsymbol{\theta}) \right],$$

from which an unbiased importance sampling estimator can be derived with the sample weights being $\frac{p(\mathbf{z}|\mathbf{x}, \boldsymbol{\theta})}{q(\mathbf{z}|\mathbf{x}; \boldsymbol{\phi})}$. However, computing $p(\mathbf{z}|\mathbf{x}, \boldsymbol{\theta})$ is often hard for most DGMs. By noticing that $p(\mathbf{z}|\mathbf{x}, \boldsymbol{\theta}) \propto p(\mathbf{x}, \mathbf{z}|\boldsymbol{\theta})$ and computing $p(\mathbf{x}, \mathbf{z}|\boldsymbol{\theta})$ is easy, we derive a self-normalized importance sampling estimate as follows:

$$\nabla_{\boldsymbol{\theta}} \log p(\mathbf{x}|\boldsymbol{\theta}) \approx \frac{\sum_{s=1}^L \left(\frac{\partial}{\partial \boldsymbol{\theta}} \log p(\mathbf{x}, \mathbf{z}^{(s)}|\boldsymbol{\theta}) \right) \cdot \omega^{(s)}}{\sum_{s=1}^L \omega^{(s)}}, \quad (6)$$

where $\{\mathbf{z}^{(s)}\}_{s=1}^L$ is a set of samples drawn from the proposal $q(\mathbf{z}|\mathbf{x}; \boldsymbol{\phi})$ and $\omega^{(s)} = \frac{p(\mathbf{x}, \mathbf{z}^{(s)}|\boldsymbol{\theta})}{q(\mathbf{z}^{(s)}|\mathbf{x}; \boldsymbol{\phi})}$ is the unnormalized likelihood ratio. This estimate is asymptotically consistent [23], and its slight bias decreases as drawing more samples.

Neural Adaptive Proposals: To reduce the variance of the estimator in Eq. (6) and get accurate gradient estimates, $q(\mathbf{z}|\mathbf{x}; \boldsymbol{\phi})$ should be as close to $p(\mathbf{z}|\mathbf{x}, \boldsymbol{\theta})$ as possible. Here, we draw inspirations from variational methods and learn adaptive proposals by minimizing some criterion. Specifically, we build a recognition model (or inference network) to represent the proposal distribution $q(\mathbf{z}|\mathbf{x}; \boldsymbol{\phi})$ of latent variables, as in the variational methods [16, 6]. Such a recognition model takes \mathbf{x} as input and outputs $\{\mathbf{z}^{(s)}\}$ as samples from $q(\mathbf{z}|\mathbf{x}; \boldsymbol{\phi})$. We optimize the quality of the proposal distribution by minimizing the inclusive KL-divergence between the target posterior distribution and the proposal $\mathbb{E}_{p(\mathbf{z}|\mathbf{x}, \boldsymbol{\theta})} [\log \frac{p(\mathbf{z}|\mathbf{x}, \boldsymbol{\theta})}{q(\mathbf{z}|\mathbf{x}; \boldsymbol{\phi})}]$ [6] or equivalently maximizing the expected log-likelihood of the recognition model

$$\mathcal{J}(\boldsymbol{\phi}; \boldsymbol{\theta}, \mathbf{x}) = \mathbb{E}_{p(\mathbf{z}|\mathbf{x}, \boldsymbol{\theta})} [\log q(\mathbf{z}|\mathbf{x}; \boldsymbol{\phi})]. \quad (7)$$

We choose this objective due to the following reasons. If the target posterior belongs to the family of proposal distributions, maximizing $\mathcal{J}(\boldsymbol{\phi}; \boldsymbol{\theta}, \mathbf{x})$ leads to the optimal solution that is the target posterior; otherwise, minimizing the inclusive KL-divergence tends to find proposal distributions that have higher entropy than the target posterior. Such a property is advantageous for importance sampling as we require that $q(\mathbf{z}|\mathbf{x}; \boldsymbol{\phi}) > 0$ wherever $p(\mathbf{z}|\mathbf{x}, \boldsymbol{\theta}) > 0$. In contrast, the exclusive KL-divergence $\mathcal{L}(\boldsymbol{\phi}; \boldsymbol{\theta}, \mathbf{x}) := \mathbb{E}_{q(\mathbf{z}|\mathbf{x}; \boldsymbol{\phi})} [\log \frac{q(\mathbf{z}|\mathbf{x}; \boldsymbol{\phi})}{p(\mathbf{z}|\mathbf{x}, \boldsymbol{\theta})}]$, as widely adopted in the variational methods [16, 25, 20], does not have such a property — It can happen that $q(\mathbf{z}|\mathbf{x}; \boldsymbol{\phi}) = 0$ when $p(\mathbf{z}|\mathbf{x}, \boldsymbol{\theta}) > 0$; therefore unsuitable for importance sampling.

The gradient of $\mathcal{J}(\boldsymbol{\phi}; \boldsymbol{\theta}, \mathbf{x})$ with respect to the parameters of the proposal distribution is

$$\nabla_{\boldsymbol{\phi}} \mathcal{J}(\boldsymbol{\phi}; \boldsymbol{\theta}, \mathbf{x}) = \mathbb{E}_{p(\mathbf{z}|\mathbf{x}, \boldsymbol{\theta})} [\nabla_{\boldsymbol{\phi}} \log q(\mathbf{z}|\mathbf{x}; \boldsymbol{\phi})], \quad (8)$$

Algorithm 1 Doubly Stochastic Gradient MCMC with Neural Adaptive Proposals

Input: \mathbf{X}

- 1: initialize θ, ϕ
- 2: **for** iteration $t = 1, 2, \dots$ **do**
- 3: sample a mini-batch $B_t \subset \{1, \dots, N\}$
- 4: **for** $i = 1$ to m of SGHMC steps **do**
- 5: sample $\{\mathbf{z}_n^{(s)}\}$ from $q(\mathbf{z}|\mathbf{x}_n; \phi), \forall n \in B_t$
- 6: estimate $\nabla \log p(\mathbf{x}_n|\theta)$ by Eq. (6), $\forall n \in B_t$
- 7: update θ by Eq. (4)
- 8: update ϕ with the gradient in Eq. (10)

Output: θ, ϕ

which can be estimated using importance sampling similar as in Eq. (6):

$$\nabla_{\phi} \mathcal{J}(\phi; \theta, \mathbf{X}) \approx \frac{\sum_{s=1}^{L'} \left(\frac{\partial}{\partial \phi} \log q(\mathbf{z}^{(s)}; \mathbf{x}, \theta) \right) \cdot \omega^{(s)}}{\sum_{s=1}^{L'} \omega^{(s)}}, \quad (9)$$

where $\{\mathbf{z}^{(s)}\}_{s=1}^{L'}$ are samples from the latest proposal distribution $q(\mathbf{z}|\mathbf{x}; \phi)$ and the weights are the same as in Eq. (6). To improve the efficiency, we adopt stochastic gradient descent methods to optimize the objective $\mathcal{J}(\phi; \theta, \mathbf{X}) := \sum_{n=1}^N \mathcal{J}(\phi; \theta, \mathbf{x}_n)$, with the gradient being estimated by a random mini-batch of data points at each iteration:

$$\nabla_{\phi} \mathcal{J}(\phi; \theta, \mathbf{X}) \approx \frac{|\mathcal{D}|}{|B_t|} \sum_{n \in B_t} \nabla_{\phi} \mathcal{J}(\phi; \theta, \mathbf{x}_n), \quad (10)$$

where each term $\nabla_{\phi} \mathcal{J}(\phi; \theta, \mathbf{x}_n)$ is further estimated by samples as in Eq. (9). This stochastic gradient descent method naturally fits into our stochastic gradient MCMC with little cost. In fact, we can use same set of samples $\{\mathbf{z}^{(s)}\}_{s=1}^{L'}$ to estimate the gradients in both Eq. (6) and Eq. (10) in practice without losing accuracy. This saves cost of drawing samples.

With the above gradient estimates, we get the overall algorithm with neural adaptive importance sampling, as outlined in Algorithm 1, where we adaptively update the proposal distribution by performing one step of recognition model update after each step of Hamiltonian dynamics simulation.

3 Sigmoid Belief Networks

We now apply the doubly stochastic gradient MCMC method to learn deep sigmoid belief networks.

A sigmoid belief network (SBN) [22] is a directed graphical model that has a generative process for binary data. Let $\mathbf{x} \in \{0, 1\}^J$ be a J -dimensional binary vector. The binary data is modeled in terms of a vector of binary hidden variables $\mathbf{z} \in \{0, 1\}^H$ by a factorized

likelihood $p(\mathbf{x}|\mathbf{z}) = \prod_{j=1}^J p(x_j = 1|\mathbf{z})$:

$$p(x_j = 1|\mathbf{z}) = \sigma(\mathbf{w}_j^{\top} \mathbf{z} + c_j), \quad (11)$$

where $\sigma(x) = 1/(1 + \exp(-x))$ is the sigmoid function and $\mathbf{W} = [\mathbf{w}_1, \dots, \mathbf{w}_J]^{\top} \in \mathbb{R}^{J \times H}$, $\mathbf{c} \in \mathbb{R}^J$ are model parameters. The prior of hidden variables is also assumed to be a factorized distribution

$$p(\mathbf{z}) = \prod_{h=1}^H p(z_h = 1) = \prod_{h=1}^H \sigma(b_h), \quad (12)$$

where $\mathbf{b} \in \mathbb{R}^H$ are the parameters. If we consider layers of SBN as ordered sequences of observed variables or hidden variables, and assume directed links within layers, we obtain an autoregressive version of SBN (ARSBN), whose prior and likelihood models are defined as follows:

$$p(z_h = 1|z_{<h}) = \sigma(\mathbf{u}_k^{\top} \mathbf{z}_{<h} + b_h), \quad (13)$$

$$p(x_j = 1|x_{<j}, \mathbf{z}) = \sigma(\mathbf{s}_{j, <j}^{\top} \mathbf{x}_{<j} + \mathbf{w}_j^{\top} \mathbf{z} + c_j), \quad (14)$$

where $\mathbf{U} = [\mathbf{u}_1, \dots, \mathbf{u}_K]^{\top}$ and $\mathbf{S} = [\mathbf{s}_1, \dots, \mathbf{s}_J]^{\top}$ are lower triangular matrices, denoting the autoregressive weights within layer.

SBN has been widely used within a deep architecture to learn latent representations [31, 21]. Recent work has been mainly focusing on developing scalable variational methods. The work [11] is an exception, which learns SBN under a Bayesian setting and employs a sparsity-inducing prior (e.g., Student-t's or the three parameter Beta normal prior [3]) on the model weights. Adopting a sparsity-inducing prior is able to bias the model toward learning sparse latent representations. However, it also makes the posterior inference challenging as the prior is non-conjugate to the sigmoid likelihood in SBN. To deal with the non-conjugacy, the very recent data augmentation techniques were applied to derive a Gibbs sampler [11]. However, this method is computationally intensive when the dataset is large and/or the number of hidden units is large. Furthermore, sampling in an augmented space can potentially lead to slow mixing rates. We will compare extensively with this strong baseline. In this paper, we use the Student-t's prior on all model parameters.

A deep sigmoid belief network (DSBN) is constructed by stacking SBN layers, with joint probability

$$p(\mathbf{x}, \mathbf{z}^{(1)}, \dots, \mathbf{z}^{(K)}) = p(\mathbf{z}^{(K)}) \prod_{l=1}^{K-1} p(\mathbf{z}^{(l)}|\mathbf{z}^{(l+1)}) p(\mathbf{x}|\mathbf{z}^{(1)}),$$

where the probability of the last (top) layer $p(\mathbf{z}^{(K)})$ follows Eq. (12) and all other factor distributions are defined as in Eq. (11) with layer-specific parameters $\theta^{(l)} = \{\mathbf{W}^{(l)}, \mathbf{c}^{(l)}\}$. Let $J^{(l)}$ be the number of units at the l -th layer (with \mathbf{x} being the 0-th layer). The model parameters for DSBN are $\theta = \{\theta^{(l)}, \mathbf{b}\}_{l=1}^K$.

It is clear that DSBN satisfies our mildest assumption of differentiability in the collapsed parameter space; therefore our doubly stochastic gradient MCMC method applies, as detailed below for both the Gibbs sampler and neural adaptive importance sampler to estimate the gradient.

For the Gibbs sampler, the goal is to draw from $p(\mathbf{z}^{(1)}, \dots, \mathbf{z}^{(K)} | \mathbf{x}, \boldsymbol{\theta})$. Note that we define $\mathbf{z}^{(0)} = \mathbf{x}$ for convenience. It iteratively draws samples from the conditional distribution of a single unit by conditioning on all other variables:

$$p(z_h^{(l)} | \mathbf{z}_{-h}^{(l)}, \mathbf{z}^{(-l)}) \propto \exp[(\mathbf{W}_{h:}^{(l)} \mathbf{z}^{(l-1)} + b_h^{(l+1)})z_h^{(l)} - \sum_{h'=1}^{J^{(l-1)}} \log(1 + e^{(\mathbf{w}_{h'}^{(l)\top} \mathbf{z}^{(l)} + c_{h'}^{(l)})}], \quad (15)$$

where $b_h^{(l)} = \mathbf{w}_h^{(l)\top} \mathbf{z}^{(l)} + c_h^{(l)}$, $\mathbf{b}^{(K+1)} = \mathbf{b}$, $\mathbf{W}_{h:}^{(l)} = [w_{1h}^{(l)}, \dots, w_{J^{(l-1)}h}^{(l)}]$, $\mathbf{z}_{-h}^{(l)}$ denotes all the variables in $\mathbf{z}^{(l)}$ except $z_h^{(l)}$, and $\mathbf{z}^{(-l)}$ denotes all the layers except $\mathbf{z}^{(l)}$. Detailed derivation is included in Appendix.

For the neural adaptive importance sampler, we construct a recognition model with the same structure as DSBN but with all layers inverted to approximate the posterior of latent layers. Specifically, we build

$$q(\mathbf{z}^{(1)}, \dots, \mathbf{z}^{(K)}; \mathbf{x}) = q(\mathbf{z}^{(1)}; \mathbf{x}) \prod_{l=1}^{K-1} q(\mathbf{z}^{(l+1)} | \mathbf{z}^{(l)}),$$

where \mathbf{x} is the input and all \mathbf{z} are sample from this inverse SBN layerstack. The parameters of the recognition model are $\boldsymbol{\phi} = \{\mathbf{W}^{(l)}, \mathbf{c}^{(l)}\}_{l=1}^K$. Note that a more complicated recognition model can lead to better performance [6]. In this paper, we restrict ourself to the simple recognition network.

4 Experiments

We now present experimental results of our doubly stochastic MCMC method on four public datasets, including **MNIST**, **Caltech-101** Silhouettes [19], **OCR** letters [17] and **MNIST8M** [18]. The MNIST and MNIST8M datasets are binarized by stochastically setting each pixel to 1 in proportion to its intensity according to [29]. Table 1 summarizes the statistics of the datasets. We use the doubly stochastic gradient Hamiltonian Monte Carlo with both a Gibbs sampler (DSGHMC-Gibbs) and an adaptive importance sampler (DSGHMC-AIS) in the experiments.

4.1 Setups

We consider five SBN models with different architectures on all the datasets. The first three are the standard SBN models — one hidden layer with 200 hidden units, two hidden layers with 200 hidden units at each layer and three hidden layers with 200 hidden units at

Table 1: The descriptions of the four datasets.

	MNIST	Caltech-101	OCR	MNIST8M
dimension	784	784	128	784
train size	50,000	4,100	32,152	8,100,000
valid size	10,000	2,264	10,000	10,100
test size	10,000	2,307	10,000	10,000

each layer. The other two are the autoregressive SBN (ARSBN) models — one has a single hidden layer with 200 units and the other one has two hidden layers with 200 units at each layer.

We compare with the recent Gibbs sampling algorithm [11] using the authors’ code, which was shown to be the best MCMC method on learning deep SBN models under Bayesian setting. The priors of model parameters are set as stated in Section 3. The model parameters are randomly initialized by sampling from an zero-mean normal with small variance. The learning rate λ_t is set among $\{0.1, 0.02, 0.01\}$, from which we report the experiment with best performance on validation set. Following the suggestion of [8], the momentum decay parameter ξ is chosen from $\{0.1, 0.05\}$. The minibatch size $|B_t|$ is set to 100 and the number of samples L during training is set to 5, which is sufficiently large for all the tested models.

For Gibbs sampling, we follow the settings in [11] (with the initial 40 epochs as burn-in). For DSGHMC-Gibbs, we use deterministic termination criteria — the number of burn-in iterations is set as 140 for one-hidden-layer, 240 for two-hidden-layer and 340 for three-hidden-layer models. The number of burn-in steps of the Gibbs sampler for the posterior of latent variables is set to 5. For DSGHMC-AIS, due to the efficiency of sampling hidden layers, we use early stopping for better convergence. The parameters of recognition model are updated using the Adam [15] optimizer with stepsizes of $\{0.001, 0.0005\}$.

ARSBN depends on the order of the input variables. In our experiments, the ordering is simply determined by the original order in the dataset. For ARSBN, we use recognition models with ARSBN layers. See Appendix for more details about the experimental setting.

4.2 Results

We present both quantitative results on predicting testing data and qualitative results on generating samples. We also analyze the time efficiency.

4.2.1 Predictive Performance

We first present predictive performance to examine the quality of posterior inference by our DSGHMC methods. To assess the quality, we report the average log-likelihood of the test data. For simplicity, one sam-

Table 2: Predictive results on various datasets, where ‘‘Dim’’ denotes the number of latent variables in each layer, with layer closest to the data laying left. Values surrounded by brackets are variational lower bounds, values without brackets are average test log-likelihoods. The results marked by * are taken from [11]. (\diamond) Discriminative fine-tuning is performed, which probably leads to better results.

Model	Dim	MNIST	Caltech-101	OCR	MNIST8M
SBN (Gibbs)	200	-115.1	-118.9	-49.5	-
SBN (Gibbs)	200-200	-102.1	-106.4	-41.8	-
SBN (VB)*	200	(-116.96)	(-136.84)	(-48.20)	-
SBN (VB)*	200-200	(-110.74) \diamond	(-125.60)	(-47.84)	-
SBN (DSGHMC-Gibbs)	200	-102.9	-116.7	-42.2	-103.2
SBN (DSGHMC-Gibbs)	200-200	-100.6	-100.8	-39.8	-101.6
SBN (DSGHMC-Gibbs)	200-200-200	-97.5	-96.3	-38.1	-97.6
SBN (DSGHMC-AIS)	200	-103.2	-128.8	-37.5	-105.8
SBN (DSGHMC-AIS)	200-200	-93.7	-114.9	-33.2	-96.4
SBN (DSGHMC-AIS)	200-200-200	-91.4	-113.6	-33.3	-93.8
ARSBN (DSGHMC-Gibbs)	200	-101.1	-101.9	-35.2	-97.9
ARSBN (DSGHMC-Gibbs)	200-200	-102.3	-104.4	-36.3	-98.3
ARSBN (DSGHMC-AIS)	200	-91.2	-110.0	-32.7	-91.4
ARSBN (DSGHMC-AIS)	200-200	-94.8	-110.8	-38.1	-93.5
ARSBN (VB)*	200	(-102.11)	(-96.78)	(-37.97)	-
ARSBN (VB)*	200-200	(-101.19)	(-97.57)	(-38.56)	-

ple drawn from the posterior after convergence is used to evaluate the results. The log-likelihoods of models trained by DSGHMC-AIS are evaluated by importance sampling according to [6] with $L = 100,000$ samples. To evaluate the models trained by DSGHMC-Gibbs, which do not have a recognition model, we adopt the Annealed Importance Sampling [29] method, which provides an unbiased estimator of the log-likelihood. We observe that the two estimators always give similar results when applying them to the same learned model (with difference less than 0.7). Details of evaluation are provided in Appendix.

Table 2 shows the average test log-likelihood on each of the four datasets, with comparison with the Gibbs sampler via data augmentation as well as the variational Bayesian (VB) [11] method for SBN and ARSBN.¹ We cite the results of VB methods from [11], which are referred as variational lower bounds.

We first examine the results for the SBN model with one hidden layer. One can observe that our method achieves similar or better results on all the datasets, compared to the Gibbs sampler. On MNIST, our method gives an average test log-likelihood of -102.9 , which brings a 12 nats improvement.

Then, we utilize a second layer for SBN. A greedy layer-wise pre-training requires generating samples of lower hidden layers as the input data for upper hidden layers. However, our method only generates a few samples for the mini-batch at each iteration, which

is not enough for pre-training the next layer. Thus pre-training is not performed in all deep models. As can be seen, utilizing a second hidden layer improves the performance on all datasets. Furthermore, our method achieves consistently better results than the Gibbs sampler. We also explore ARSBNs with one hidden layer and two hidden layers. Our method on autoregressive structures give improvements compared to standard SBN as expected, which suggests that our method works on different deep generative models.

We further investigate the performance of SBN models with three hidden layers. Training such models using Gibbs sampling is too time-costly and thus is not included in Table 2. We can see that our method continues improving the results as the model grows deeper, which shows that our methods scale better to large or deep structures than Gibbs sampling.

Table 3 shows comparison on MNIST results of various training methods, including Neural Variational Inference and Learning (NVIL) [20], wake-sleep [12] and Reweighted Wake-Sleep (RWS) [6]. Our method gives better results than wake-sleep and achieves comparable results with RWS(Q:SBN), which uses a same recognition model as ours to approximate the posterior of latent variables.

We observe that on MNIST and OCR (See Table 2), DSGHMC-AIS gives better results than DSGHMC-Gibbs, while on Caltech-101 the facts are the opposite. Note that depending on the dataset being modeled, a Gibbs sampler for posterior of latent variables can give poor samples when it has a low mixing rate,

¹For ARSBN, the work [11] only reported the results with variational Bayes.

Table 3: MNIST results of various training methods on SBNs with various architectures. The results of NVIL are cited from [20]; and the results of Wake-sleep and RWS are cited from [6].

Model	Dim	Variational Bayes			MCMC		
		NVIL	wake-sleep	RWS(Q:SBN)	Gibbs	DSGHMC-Gibbs	DSGHMC-AIS
SBN	200	(-113.1)	-116.3(-120.7)	-103.1	-115.1	-102.9	-103.2
SBN	200-200	(-99.8)	-106.9(-109.4)	-93.4	-102.1	-100.6	-93.7
SBN	200-200-200	(-96.7)	-101.3(-104.4)	-90.1	-	-97.5	-91.4

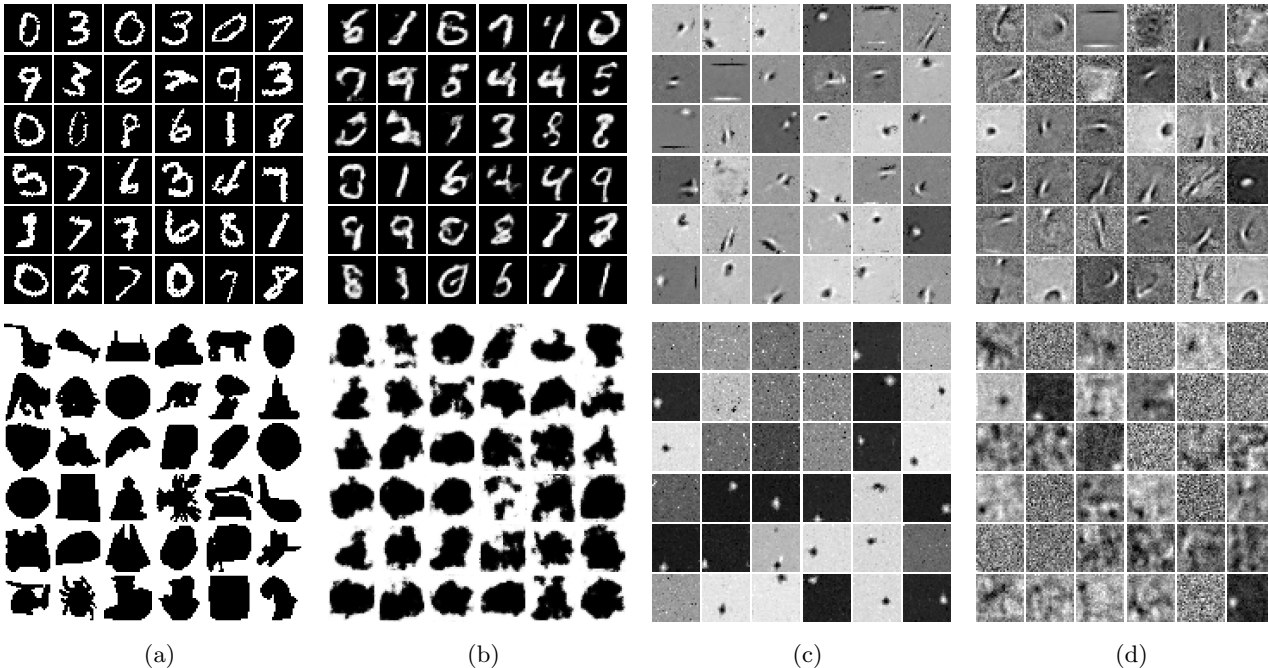


Figure 1: Visualization: (a) Training data. (b) Samples from the SBN(200-200-200) model. (The probabilities for sampling each pixel are showed.) (c) Features at the bottom layer learned with sparse prior. (d) Features at the bottom layer learned with normal prior. (Top) MNIST. (Bottom) Caltech-101.

while a neural adaptive importance sampler can give poor samples when true posterior is far from the scope a recognition model can approximate. Thus depending on the different datasets being modeled, either one of above may become dominating, leading to the different performance of the two proposed methods. Using a more powerful recognition model may further improve the performance of DSGHMC-AIS [6]; We leave a systematic investigation as our future work.

Finally, our efficient DSGHMC methods manage to learn the deep SBN models on the large-scale MNIST8M [18] dataset, which consists of 8.1 million training digit images generated by applying transformation to the standard MNIST training examples and has a same testing set as the standard MNIST dataset. MNIST8M is too large to be processed by the batch Gibbs sampler. Again, we can see in Table 2 that by increasing the model depth the testing log-likelihoods improve for SBN models. The slightly worse results for ARSBN may be due to overfitting.

4.2.2 Generative Performance

Fig. 1 shows the generative ability of the learned SBN models. In Fig. 1(a), we show the randomly sampled training data of MNIST and Caltech-101. Fig. 1(b) presents some random examples generated from 3-layer SBNs learned by DSGHMC-AIS.

One advantage of Bayesian framework is that we can specify some sparsity-encouraging priors on the model parameters explicitly, e.g., Student-t prior in our experiments. Fig. 1(c) and Fig. 1(d) demonstrate the difference between features learned with sparse priors and non-sparse priors. We can see that the features learned with sparse priors appear more localized.

We further examine the ability of the learned models on predicting missing data. For each test image, the lower half is assumed missing and the upper half is used to inference the hidden units [11]. Then, with the hidden units, the lower half is constructed. Prediction is done by repeating this procedure and adopting a majority vote for each pixel. Fig. 2 demonstrates some example completions for the missing data on MNIST.

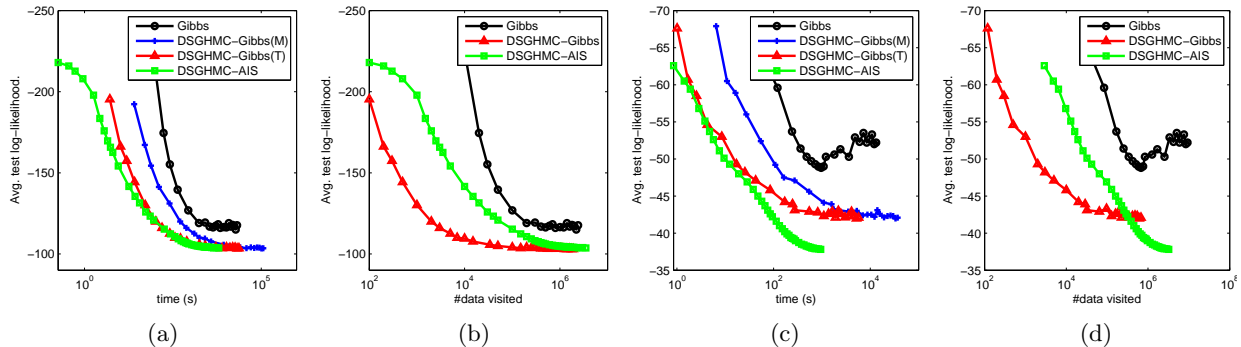


Figure 3: Convergence curves with respect to training time and number of training data visited on (a-b) MNIST and (c-d) OCR letters datasets. In (a) and (c) DSGHMC-Gibbs(T) denotes DSGHMC-Gibbs implemented in Theano with GPU acceleration and DSGHMC-Gibbs(M) denotes DSGHMC-Gibbs in MATLAB code.

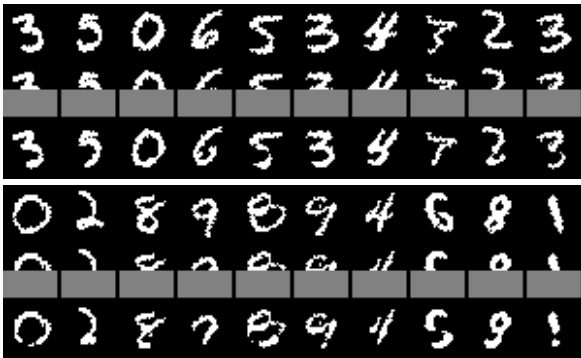


Figure 2: Missing data prediction: (Top) Original data. (Middle) Hollowed data. (Bottom) Reconstructed data.

4.2.3 Time Efficiency

We compare the efficiency of Gibbs, DSGHMC-Gibbs and DSGHMC-AIS in this section. We implement both DSGHMC-Gibbs and DSGHMC-AIS in Theano [4] with GPU acceleration. For fair comparison with Gibbs (MATLAB code by [11]), we also implement DSGHMC-Gibbs in MATLAB code. Table 4 presents the efficiency of Gibbs and DSGHMC-Gibbs on different datasets. We can see that DSGHMC-Gibbs is faster than the Gibbs sampler on all the four datasets, especially for the large-scale MNIST8M dataset, which is too time-consuming for the Gibbs sampler. Note that our DSGHMC-Gibbs spends almost identical time at each iteration on MNIST, Caltech-101 and MNIST8M datasets, due to the fact that all these datasets have the same dimensionality, which shows the scalability of the proposed method.

We gain significant acceleration by using GPU. For example, On MNIST, the average training time (one-hidden-layer SBN) per iteration of DSGHMC-Gibbs and DSGHMC-AIS is 5.2s and 0.18s, respectively.

Fig. 3 shows the convergence curves on the MNIST and OCR datasets with respect to the training time and the number of training data visited. We can see

Table 4: Average training time per iteration using Gibbs and DSGHMC-Gibbs for one-hidden-layer SBN (200 hidden units). Experiments in this table are conducted using MATLAB code for both methods on a PC with eight Intel Core i7-4770 CPUs (3.40GHz).

Datasets	train-size	Gibbs	DSGHMC-Gibbs
MNIST	50,000	405.6s	25.4s
Caltech-101	4,100	36.1s	25.4s
OCR	32,152	45.8s	5.44s
MNIST8M	8,100,000	> 10h	25.6s

that: 1) Both DSGHMC-Gibbs and DSGHMC-AIS converge faster and better than Gibbs; 2) both methods visit fewer data points to converge, compared to Gibbs; and 3) DSGHMC-AIS converges faster than DSGHMC-Gibbs with respect to training time.

5 Conclusions and Future Work

We present doubly stochastic gradient MCMC, a simple and general method, to learn deep generative models in a Bayesian setting. When applied to deep sigmoid belief networks, our method manages to learn on large-scale datasets with good inference accuracy.

For future work, we like to apply this method to learn even deeper belief networks. We are also interested in investigating the performance on learning sparse Bayesian models, which often involve intractable gradients that can be estimated by our doubly stochastic strategy. Finally, learning nonparametric Bayesian DGMS is another interesting challenge.

References

- [1] R. Adams, H. Wallach, and Z. Ghahramani. Learning the structure of deep sparse graphical models. In *AISTATS*, 2010.
- [2] S. Ahn, A. Korattikara, and M. Welling. Bayesian posterior sampling via stochastic gradient fisher scoring. In *ICML*, 2012.

-
- [3] A. Armagan, D. Dunson, and M. Clyde. Generalized beta mixtures of gaussians. In *NIPS*, pages 523–531, 2011.
- [4] F. Bastien, P. Lamblin, R. Pascanu, J. Bergstra, I. Goodfellow, A. Bergeron, N. Bouchard, D. Warde-Farley, and Y. Bengio. Theano: new features and speed improvements. Deep Learning and Unsupervised Feature Learning NIPS 2012 Workshop, 2012.
- [5] Y. Bengio, E. Laufer, G. Alain, and J. Yosinski. Deep generative stochastic networks trainable by backprop. In *ICML*, 2014.
- [6] J. Bornschein and Y. Bengio. Reweighted wake-sleep. *CoRR*, abs/1406.2751, 2014.
- [7] L. Bottou. *Online Algorithms and Stochastic Approximations*. Online Learning and Neural Networks, Edited by David Saad, Cambridge University Press, Cambridge, UK, 1998.
- [8] T. Chen, E. Fox, and C. Guestrin. Stochastic gradient Hamiltonian Monte Carlo. In *ICML*, 2014.
- [9] N. Ding, Y. Fang, R. Babbush, C. Chen, and H. Skeel, R. and Neven. Bayesian sampling using stochastic gradient thermostats. In *NIPS*, pages 3203–3211, 2014.
- [10] Z. Gan, C. Chen, R. Henao, D. Carlson, and L. Carin. Scalable deep poisson factor analysis for topic modeling. In *ICML*, 2015.
- [11] Z. Gan, R. Henao, D. Carlson, and L. Carin. Learning deep sigmoid belief networks with data augmentation. In *AISTATS*, 2015.
- [12] G. E. Hinton, P. Dayan, B. J. Frey, and R. M. Neal. The “wake-sleep” algorithm for unsupervised neural networks. *Science*, 268(5214):1158–1161, 1995.
- [13] G. E. Hinton, S. Osindero, and Y. Teh. A fast learning algorithm for deep belief nets. *Neural Computation*, 18, 2006.
- [14] M. Jordan, Z. Ghahramani, T. Jaakkola, and L. Saul. An introduction to variational methods for graphical models. *MLJ*, 37(2):183–233, 1999.
- [15] D. P. Kingma and J. Ba. Adam: A method for stochastic optimization. *CoRR*, abs/1412.6980, 2014.
- [16] D. P. Kingma and M. Welling. Auto-encoding variational bayes. In *ICLR*, 2014.
- [17] M. Lichman. UCI machine learning repository, 2013.
- [18] G. Loosli, S. Canu, and L. Bottou. Training invariant support vector machines using selective sampling. In L. Bottou, O. Chapelle, D. DeCoste, and J. Weston, editors, *Large Scale Kernel Machines*, pages 301–320. MIT Press, Cambridge, MA., 2007.
- [19] B. Marlin, K. Swersky, B. Chen, and N. Freitas. Inductive principles for restricted boltzmann machine learning. In *AISTATS*, pages 509–516, 2010.
- [20] A. Mnih and K. Gregor. Neural variational inference and learning in belief networks. In *ICML*, 2014.
- [21] A. Mohamed, G. Dahl, and G. Hinton. Acoustic modeling using deep belief networks. *IEEE Trans. on Audio, Speech, and Language Processing*, 20(1):14–22, 2012.
- [22] R. Neal. Connectionist learning of belief networks. *Artif. Intell.*, 56(1):71–113, 1992.
- [23] A. B. Owen. *Monte Carlo theory, methods and examples*. 2013.
- [24] S. Patterson and Y. Teh. Stochastic gradient Riemannian Langevin dynamics on the probability simplex. In *NIPS*, 2013.
- [25] D. J. Rezende, S. Mohamed, and D. Wierstra. Stochastic backpropagation and approximate inference in deep generative models. In *ICML*, 2014.
- [26] H. Robbins and S. Monro. A stochastic approximation method. *The Annals of Mathematical Statistics*, 22(3):400–4007, 1951.
- [27] C. Robert and G. Casella. *Monte Carlo Statistical Methods*. Springer, 2005.
- [28] R. Salakhutdinov and G. E. Hinton. Deep Boltzmann machines. In *AISTATS*, 2009.
- [29] R. Salakhutdinov and I. Murray. On the quantitative analysis of deep belief networks. In *ICML*, pages 872–879, 2008.
- [30] L. Saul, T. Jaakkola, and M. Jordan. Mean field theory for sigmoid belief networks. *Journal of AI Research*, 4:61–76, 1996.
- [31] I. Titov and J. Henderson. Constituent parsing with incremental sigmoid belief networks. In *ACL*, 2007.
- [32] M. Welling and Y. Teh. Bayesian learning via stochastic gradient Langevin dynamics. In *ICML*, 2011.

Appendix

In this appendix, we first provide the derivations of the Gibbs sampler for DSGHMC-Gibbs. We also give details about how we evaluate the learned models. Finally we show some extra experimental settings.

A Derivations

A.1 Gibbs sampler for DSBN latent layers

We sample the latent variables layer by layer and dimension-wise within each layer. Note that we define $\mathbf{z}^{(0)} = \mathbf{x}$ for convenience. Then $p(z_h^{(l)} | \mathbf{z}_{-h}^{(l)}, \mathbf{x}, \mathbf{z}^{(-l)})$ can be written as $p(z_h^{(l)} | \mathbf{z}_{-h}^{(l)}, \mathbf{z}^{(-l)})$. We have

$$\begin{aligned}
& p(z_h^{(l)} | \mathbf{z}_{-h}^{(l)}, \mathbf{z}^{(-l)}) \\
&= p(z_h^{(l)} | \mathbf{z}_{-h}^{(l)}, \mathbf{z}^{(<l)}, \mathbf{z}^{(>l)}) \\
&\propto p(\mathbf{z}^{(<l)} | z_h^{(l)}, \mathbf{z}_{-h}^{(l)}, \mathbf{z}^{(>l)}) \cdot p(z_h^{(l)} | \mathbf{z}_{-h}^{(l)}, \mathbf{z}^{(>l)}) \\
&= p(\mathbf{z}^{(<l)} | \mathbf{z}^{(l)}) \cdot p(z_h^{(l)} | \mathbf{z}^{(l+1)}) \\
&= p(\mathbf{z}^{(l-1)} | \mathbf{z}^{(l)}) \cdot p(\mathbf{z}^{(<l-1)} | \mathbf{z}^{(l-1)}, \mathbf{z}^{(l)}) \cdot p(z_h^{(l)} | \mathbf{z}^{(l+1)}) \\
&\propto p(\mathbf{z}^{(l-1)} | \mathbf{z}^{(l)}) \cdot p(z_h^{(l)} | \mathbf{z}^{(l+1)}) \\
&= \prod_{h'=1}^{J^{(l-1)}} \exp \left[(\mathbf{w}_{h'}^{(l)\top} \mathbf{z}^{(l)} + c_{h'}^{(l)}) z_{h'}^{(l-1)} \right. \\
&\quad \left. - \log(1 + e^{(\mathbf{w}_{h'}^{(l)\top} \mathbf{z}^{(l)} + c_{h'}^{(l)})}) \right] \\
&\quad \times \exp \left[(\mathbf{w}_h^{(l+1)\top} \mathbf{z}^{(l+1)} + c_h^{(l+1)}) z_h^{(l)} \right. \\
&\quad \left. - \log(1 + e^{(\mathbf{w}_h^{(l+1)\top} \mathbf{z}^{(l+1)} + c_h^{(l+1)})}) \right] \\
&\propto \exp \left[\left(\sum_{h'=1}^{J^{(l-1)}} W_{h'h}^{(l)} z_{h'}^{(l-1)} + (\mathbf{w}_h^{(l+1)\top} \mathbf{z}^{(l+1)} + c_h^{(l+1)}) \right) z_h^{(l)} \right. \\
&\quad \left. - \sum_{h'=1}^{J^{(l-1)}} \log(1 + e^{(\mathbf{w}_{h'}^{(l)\top} \mathbf{z}^{(l)} + c_{h'}^{(l)})}) \right].
\end{aligned}$$

For $l = K$, there is no upper layers and the term $\mathbf{w}_h^{(l)\top} \mathbf{z}^{(l)} + c_h^{(l)}$ which is denoting the confidence from upper layer will be replaced with the prior of the top layer b_h . We define $\mathbf{W}_{h:}^{(l)} = [w_{1h}^{(l)}, \dots, w_{J^{(l-1)}h}^{(l)}]$, $b_h^{(l)} = \mathbf{w}_h^{(l)\top} \mathbf{z}^{(l)} + c_h^{(l)}$ and $b_h^{(K+1)} = b_h$ for notational convenience. Finally we get Eq. (15)

$$\begin{aligned}
p(z_h^{(l)} | \mathbf{z}_{-h}^{(l)}, \mathbf{z}^{(-l)}) &\propto \exp[(\mathbf{W}_{h:}^{(l)} \mathbf{z}^{(l-1)} + b_h^{(l+1)}) z_h^{(l)} \\
&\quad - \sum_{h'=1}^{J^{(l-1)}} \log(1 + e^{(\mathbf{w}_{h'}^{(l)\top} \mathbf{z}^{(l)} + c_{h'}^{(l)})})],
\end{aligned}$$

for $l = 1$ to K .

A Gibbs sampler of DARSBN can be derived in a similar way.

B Evaluation

In our experiment, all models are evaluated in terms of average test log-likelihood. We now present the details of evaluation.

B.1 Importance sampling

For the models trained by DSGHMC-AIS, we can evaluate the log-likelihood using importance sampling [6]. Specifically, we have an unbiased estimator

$$\begin{aligned}
p(\mathbf{x} | \boldsymbol{\theta}) &= \mathbb{E}_{p(\mathbf{z} | \mathbf{x}, \boldsymbol{\theta})} [p(\mathbf{x} | \boldsymbol{\theta})] \\
&= \mathbb{E}_{q(\mathbf{z} | \mathbf{x}; \boldsymbol{\phi})} \left[\frac{p(\mathbf{z} | \mathbf{x}, \boldsymbol{\theta})}{q(\mathbf{z} | \mathbf{x}; \boldsymbol{\phi})} p(\mathbf{x} | \boldsymbol{\theta}) \right] \\
&\approx \frac{1}{L} \sum_{s=1}^L \frac{p(\mathbf{x}, \mathbf{z}^{(s)} | \boldsymbol{\theta})}{q(\mathbf{z}^{(s)} | \mathbf{x}; \boldsymbol{\phi})}, \tag{16}
\end{aligned}$$

where $\{\mathbf{z}^{(s)}\}_{s=1}^L$ are samples from the proposal distribution $q(\mathbf{z} | \mathbf{x}; \boldsymbol{\phi})$. In the experiments, we take the logarithm of the above estimator to compute the log-likelihood. Note that taking logarithm makes the estimator biased [6], but the bias and the variance will decrease as the number of samples L increase. In our experiments, we use $L = 100,000$, which is shown sufficiently large.

B.2 Annealed importance sampling

For the models trained by DSGHMC-Gibbs or the Gibbs sampling [11], the above estimator is not applicable since no recognition model is trained. Noticing $p(\mathbf{z} | \mathbf{x}, \boldsymbol{\theta}) = p(\mathbf{x}, \mathbf{z} | \boldsymbol{\theta}) / p(\mathbf{x} | \boldsymbol{\theta})$, we can view $p(\mathbf{x}, \mathbf{z} | \boldsymbol{\theta})$ as some unnormalized probability of $p(\mathbf{z} | \mathbf{x}, \boldsymbol{\theta})$ and the $p(\mathbf{x} | \boldsymbol{\theta})$ as the normalizing constant. We adopt the Annealed Importance Sampling (AIS) [29] method, which can evaluate the ratio of normalizing constants accurately by reducing the variance of estimation via a sequence of intermediate distributions. See [29] for details.

For our DSBN, we leverage the AIS to compute the likelihood $p(\mathbf{x} | \boldsymbol{\theta})$ by computing the ratio of $p(\mathbf{x} | \boldsymbol{\theta})$ and $p(\mathbf{x} | \boldsymbol{\theta} = \mathbf{0})$, where $p(\mathbf{x} | \boldsymbol{\theta} = \mathbf{0})$ is the likelihood with all model parameters being 0. Note that $\boldsymbol{\theta} = \mathbf{0}$ implies the likelihood is a constant $p(\mathbf{x} | \boldsymbol{\theta} = \mathbf{0}) = 2^{-J^{(0)}}$ where $J^{(0)}$ is the dimension of \mathbf{x} , since each dimension of \mathbf{x} has equal probability to be 0 or 1. Thus computing the ratio $\frac{p(\mathbf{x} | \boldsymbol{\theta})}{p(\mathbf{x} | \boldsymbol{\theta} = \mathbf{0})}$ is equivalent to computing the likelihood $p(\mathbf{x} | \boldsymbol{\theta})$.

To compute the ratio, we introduce a sequence of intermediate distribution with $p_0(\mathbf{z}) = p(\mathbf{z}, \mathbf{x} | \boldsymbol{\theta} =$

$\mathbf{0}$), \dots , $p_k(\mathbf{z}) = p(\mathbf{z}, \mathbf{x} | \frac{k}{K}\boldsymbol{\theta})$, \dots , $p_K(\mathbf{z}) = p(\mathbf{x}, \mathbf{z} | \boldsymbol{\theta})$ for $k = 0, \dots, K$, where K is the number of intermediate distributions and $\frac{k}{K}\boldsymbol{\theta}$ denotes model parameters multiplied by $\frac{k}{K}$. Then we estimate $\frac{p(\mathbf{x}|\boldsymbol{\theta})}{p(\mathbf{x}|\boldsymbol{\theta}=\mathbf{0})}$ by

$$\frac{p_1(\mathbf{z}_1) p_2(\mathbf{z}_2) \dots p_{K-1}(\mathbf{z}_{K-1}) p_K(\mathbf{z}_K)}{p_0(\mathbf{z}_1) p_1(\mathbf{z}_2) \dots p_{K-2}(\mathbf{z}_{K-1}) p_{K-1}(\mathbf{z}_K)}, \quad (17)$$

where \mathbf{z}_0 is sampled from $p_0(\mathbf{z})$, and \mathbf{z}_{k+1} is sampled from the Gibbs sampler Eq. (15) with assumption that the current latent layers is \mathbf{z}_k and the model is $\frac{k}{K}\boldsymbol{\theta}$.

In our experiments we choose $K = 1000$ and evaluate the log-likelihood by computing Eq. (17) repeatedly and taking average.

C More Detailed Experimental Settings

In Eq. (4), the gradient $\nabla_{\boldsymbol{\theta}}U(\boldsymbol{\theta})$ is depending on the size of data, which results the fact that for different datasets we have to choose different learning rates. In our experiments, instead of evaluating the summation of the gradient among all the data \mathbf{x}_n , we compute the ‘‘per-data gradient’’ $\nabla_{\boldsymbol{\theta}}U(\boldsymbol{\theta})/|\mathcal{D}|$ in order to use same learning rate. For the majority of our experiments a learning rate 0.01 give the best results.

One parameter not mentioned in the main paper is the number of discretization steps when simulating the dynamics. In our experiments, we fixed the number of steps to 10.

The Student-t’s prior used in the experiments are set with a scale parameter $\sigma = 0.09$, location parameter $\mu = 0$ and degrees of freedom $\nu = 2.2$.